STEM CELLS TRANSLATIONAL MEDICINE®

TISSUE-SPECIFIC PROGENITOR AND STEM CELLS

Skin-Derived Precursors as a Source of Progenitors for Corneal Endothelial Regeneration

EMI INAGAKI,[a] SHIN HATOU,[a] KAZUNARI HIGA,[b] SATORU YOSHIDA,[a] SHINSUKE SHIBATA,[c] HIDEYUKI OKANO,[c] KAZUO TSUBOTA,[a] SHIGETO SHIMMURA[a]

Key Words. Corneal endothelium • Cornea • Neural crest • Skin progenitors • Cell culture

[a]Department of Ophthalmology, Keio University School of Medicine, Tokyo, Japan; [b]Department of Ophthalmology, Tokyo Dental College Ichikawa General Hospital, Ichikawa, Japan; [c]Department of Physiology, Keio University School of Medicine, Tokyo, Japan

Correspondence: Shigeto Shimmura, M.D., Department of Ophthalmology, Keio University School of Medicine, 35 Shinano-machi, Shinjuku-ku, Tokyo 160-8582, Japan. Telephone: 81-3-3358-5962; Fax: 81-3-3359-8302; e-mail: shige@z8.keio.jp

Received 28 March 2016; accepted for publication 30 September 2016; published Online First on 6 February 2017.

1066-5099/2017/$30.00/0

http://dx.doi.org/10.1002/sctm.16-0162

ABSTRACT

Corneal blindness is the fourth leading cause of blindness in the world. Current treatment is allogenic corneal transplantation, which is limited by shortage of donors and immunological rejection. Skin-derived precursors (SKPs) are postnatal stem cells, which are self-renewing, multipotent precursors that can be isolated and expanded from the dermis. Facial skin may therefore be an accessible autologous source of neural crest derived cells. SKPs were isolated from facial skin of Wnt1-Cre/Floxed EGFP mouse. After inducing differentiation with medium containing retinoic acid and GSK 3-β inhibitor, SKPs formed polygonal corneal endothelial-like cells (sTECE). Expression of major corneal endothelial markers were confirmed by Reverse transcription polymerase chain reaction (RT-PCR) and quantitative Real time polymerase chain reaction (qRT-PCR). Western blots confirmed the expression of Na, K-ATPase protein, the major functional marker of corneal endothelial cells. Immunohistochemistry revealed the expression of zonular occludens-1 and Na, K-ATPase in cell-cell junctions. In vitro functional analysis of Na, K-ATPase pump activity revealed that sTECE had significantly high pump function compared to SKPs or control 3T3 cells. Moreover, sTECE transplanted into a rabbit model of bullous keratopathy successfully maintained corneal thickness and transparency. Furthermore, we successfully induced corneal endothelial-like cells from human SKPs, and showed that transplanted corneas also maintained corneal transparency and thickness. Our findings suggest that SKPs may be used as a source of autologous cells for the treatment of corneal endothelial disease. © STEM CELLS TRANSLATIONAL MEDICINE *2017;6:788–798*

SIGNIFICANCE STATEMENT

Corneal endothelial dysfunction is a common cause of corneal blindness. Our work describes how functional corneal endothelial cells can be derived from neural crest cells isolated from facial skin (SKPs) of mice and humans. SKPs can be isolated from surgically removed redundant skin, suggesting that they can be used as an autologous source for regenerating the cornea.

INTRODUCTION

The corneal endothelium is a monolayer of cells covering the inner surface of the cornea. It plays a physiological role in maintaining cornea transparency by pump and barrier functions [1]. Corneal endothelium has limited proliferative capacity in vivo [2]. The average density of endothelial cells in neonates is 3500–4000 cells per mm^2, whereas the average in adults is 2000 cells per mm^2 [2]. The cell density continues to decrease gradually throughout life due to aging [3], and cell loss is accelerated after trauma, cataract surgery, or genetically based diseases such as Fuchs corneal dystrophy [4, 5]. Decompensation of the corneal endothelium may occur under a cell density of 500 cells per mm^2. This results in corneal stromal edema called bullous keratopathy. Corneal blindness is the fourth leading cause of blindness in the world, of which half is due to corneal endothelial dysfunction [6]. Allogenic corneal transplantation is the most common cure for corneal blindness [5]. However, there is a shortage of donor corneas worldwide, and graft failure, immunological rejection and complications such as secondary glaucoma are major complications [7, 8].

We previously reported that progenitors derived from the corneal stroma (COPs: Cornea-derived progenitor cells) could be induced to differentiate into functional corneal endothelial cells [9]. However, access to human COPs is limited due to the small size of the cornea, as well as the limited proliferative capacity. Using autologous COPs is also unreasonable due to irreversible damage to the donor eye. We therefore hypothesized that facial skin may be used as an alternative accessible, autologous source of neural crest cells, which may be able to differentiate into corneal endothelium. Skin-derived precursors (SKPs) are self-renewing, multipotent precursors that are isolated

and expanded from the dermis of rodents and human [10, 11]. SKPs share characteristics with embryonic neural crest stem cells, and are reported to differentiate into neural crest derived cell types such as Schwann cells [12, 13], and mesenchymal cells such as skeletogenic cells, adipocytes, and dermal fibroblasts [10, 11, 14, 15]. The persistence of neural crest-related precursors within accessible postnatal tissues raises the possibility of their use for variety of research and therapeutic purposes [16–18]. One example is the use of SKPs to generate myelinating Schwann cells for treating injured and demyelinated nerves [12, 19]. Successful cutaneous nerve regeneration was also demonstrated [20]. Of particular importance to our study, lineage-tracing experiments showed that SKPs isolated from facial skin are derived from the neural crest, while SKPs from dorsal skin are of somatic origin [15, 21].

The corneal endothelium also originates from neural crest cells that migrate to the cornea during embryogenesis [22, 23]. Expression of the homeobox gene, *Pitx2* is required for ocular anterior segment development [24]. In this study, we first demonstrated how tissue engineered corneal endothelium derived from mouse and human facial SKPs exhibit corneal endothelial gene and protein expression, including *Pitx2*. We then assessed whether SKPs derived tissue engineered corneal endothelium (sTECE) has Na, K-ATPase pump function equivalent to native corneal endothelium using the Ussing chamber [25]. Finally, we also show how sTECE maintains corneal transparency and thickness in a rabbit model of bullous keratopathy in vivo.

Materials and Methods

Animals

Transgenic mice expressing Cre recombinase under control of the Wnt1 promoter/ enhancer (Wnt1-Cre) [26] were mated with enhanced green fluorescent protein reporter mice (CAG-CAT-EGFP) [27] to obtain Wnt1-Cre/ Floxed-EGFP double-transgenic mice. Wild-type mice (C57BL6/J Jcl) mouse were purchased from (CLEA Japan, Inc., Tokyo, Japan, http://www.clea-japan.com/en). All animals were handled in full accordance with the Association for Research in Vision and Ophthalmology (ARVO) Statement for the Use of Animals in Ophthalmic and Vision Research. This study was approved by the Committee for Animal Research of Keio University School of Medicine (Approval Number: 08050-16) and Tokyo Dental College Ichikawa General Hospital (Approval Number: 257407).

Cell Culture

Murine SKPs were isolated from mouse skin as described previously with minor modifications [10, 28]. In brief, facial skin from mouse neonates (P1–P7) were carefully dissected free of other tissue, cut into 5 mm pieces, washed three times in Hank's balanced salt solution, (ThermoFisher Scientific, Waltham, MA, https://www.thermofisher.com) and then tissues were incubated in a 2 mg/ml solution of dispase II (Roche Applied Science, Penzberg Germany, http://www.roche-applied science.com) at 4°C overnight. After the epidermis was peeled off of the underlying dermis, dissected tissue pieces were minced into 1–2 mm pieces and then digested with 1mg/ml of type I collagenase (Wako Pure Chemical Industries, Osaka, Japan, http://www.wako-chem.co.jp/english) at 37°C for 60 minutes. Tissue pieces were then washed twice with DMEM: F12 (NACALAI TESQUE, INC. Kyoto, Japan, http://www.nacalai.com) and mechanically dissociated and the suspension poured through a 40-μm cell strainer (Falcon, Corning, Corning, NY, http://www.corning.com) to remove remaining tissue pieces. Dissociated cells were centrifuged at 170*g* and suspended in SKPs proliferation medium consisting of Dulbecco's modified Eagle's medium (DMEM)/F12 3:1 + glutamax containing medium (Gibco, Themofisher Scientific Inc.) with 2% B-27 (Gibco, Themofisher Scientific Inc.), 20 ng/ml of EGF (Pepro Tech Inc., Rocky Hill, NJ, http://www.peprotech.com) and 40 ng/ml of bFGF (Pepro Tech Inc), 1 mg/ml of Penicillin/streptomycin (Cambrex Corporation, East Rutherfold, NJ http://www.cambrex.com), and 1% Fungizone (Gibco, Themofisher Scientific Inc.).

Cells were cultured in low cell binding 6-well culture plates (Greiner-Bio-One, Kremsmünster, Australia, https://www.gbo.com/en_INT.html) in a 37°C, 5% CO_2 tissue-culture incubator. Under these conditions, SKPs proliferated as floating spheres. In order to passage the cells, spheres were centrifuged at 170*g* for 5 minutes. Pellets were then incubated with Accumax (Innovative Cell Technologies, San Diego, CA, http://www.accutase.com) for 10 minutes and mechanically dissociated to single cells with vigorous trituration by p-1000 pipette and washed three times by DMEM-F12. SKPs were passaged every 7–14 days, and SKPs at passage 2–5 were used for experiments.

NIH/3T3 cells were purchased from American Type Culture Collection (ATCC, Manassas, Virginia, http://www.atcc.org) and cultured with DMEM (NACALAI TESQUE, INC.) containing 10% FBS. Mouse corneal endothelial cells (mCE) were obtained from adult 8 to 10-week-old C57BL6/J Jcl wild type mice. After the mice were sacrificed, eyes were enucleated, and the globes were rinsed with sterile PBS. Then, the corneas were dissected from the globe, and the endothelial layer with Descemet's membrane was stripped under a dissecting microscope (SZ61, Olympus Corporation. Tokyo, Japan, http://www.olympus-global.com). Primary cultures were maintained in DMEM/F12 supplemented with 20 ng/ml of EGF, 10 ng/ml of FGF-2, B27 supplement (Gibco, Thermo Fisher Scientific), 10^3 U/ml leukemia inhibitory factor (Chemicon International, Inc. Temecula, CA, http://chemicon.com) and 10% FBS. mCE at passage 2-3 were used for experiments.

Human corneal endothelial cell line (B4G12) which were immortalized by SV40 large T- and small T-antigens, were purchased from DSMZ (Braunschweig, Germany, https://www.dsmz.de/), and cultured in Human-Endothelial-SFM (Gibco, Thermo Fisher Scientific, Inc.), supplemented with 1.0% fetal bovine serum and 10 ng/ml FGF2 under a humidified atmosphere of 5% CO_2 at 37°C. The medium was changed every 2 to 3 days. B4G12 cells reached semi-confluence in a week, were replated on 35-mm dishes, Snapwell inserts, or type 1 atelocollagen sheets (CM6, Koken, Tokyo, Japan, http://www.kokenmpc.co.jp/), and were cultured for subsequent experiments.

Human SKPs (hSKPs) were isolated from eyelid skin of individuals undergoing ocular plastic surgery for blepharochalasis, a condition caused by aging where redundant skin is removed surgically. Samples were collected following written informed consents, and the study was performed in adherence to the Declaration of Helsinki. All experiments were approved by the institutional IRB (Approval Number: 2011-221-2). Skin samples were taken from 2 male and 2 female patients (mean age 61 ± 21.51 years old). Initial culture of hSKPs was done according to method described with mice. Briefly, after fat tissues were removed, the dermis was dissociated in collagenase, and then cells we seeded in low cell-binding culture plates (Greiner Bio-One) for 1 week. Adherent culture of SKPs was performed according to the method reported in

previous report [29–31]. Initial adherent culture was performed in 25-cm^2 culture flasks and expanded into 75-cm^2 culture flasks for two to five passages in SKPs proliferation medium with the addition of 5% FBS. Cells were passaged every 3–4 days, and medium was changed every 2–3 days. After expansion in 75-cm^2 culture flasks, hSKPs were cultured into low cell binding culture plates for 7 days prior to differentiation.

In Vitro Differentiation

To examine endothelial cell differentiation, we modified our previous protocol [9]. Briefly, murine SKPs were collected and plated at a density of 2×10^5 cells per centimeter on 0.1% gelatin-coated 35-mm dishes. Cells were cultured for 1 week in Corneal Endothelium Inducing Medium (CEIM) consisting of Eagle's minimum essential medium (MEM; Sigma-Aldrich, St. Louis, MO, http://www.sigmaaldrich.com) supplemented with 5% fetal bovine serum (Sigma-Aldrich), 1% Insulin, Transferrin, Selenium Solution (ITS -G) (Sigma-Aldrich), 1 mM all-trans retinoic acid (Sigma-Aldrich), 0.5 mM BIO (glycogen synthase kinase 3β inhibitor) (Merck Milliore, Darmstadt, Germany, http://www.merkmillipore.com), 5 ng/ml transforming growth factor β2 (Pepro Tech Inc), 10 μM Y-27632 (NACALAI TESQUE, INC), 1 mM insulin (Sigma-Aldrich), 1 mM $CaCl_2$ (Sigma-Aldrich), 1mM sodium pyruvate (Sigma-Aldrich), 100 U/ml penicillin Minimum Essential Medium (MEM) (Sigma-Aldrich), 100 mg/ml streptomycin (Sigma-Aldrich), amino acid (Sigma-Aldrich) and MEM essential vitamin mixture (Bio Whittaker, Lonza, Basel, Switzerland, http://www.lonza.com). The cells were cultured for 1 week under a humidified atmosphere of 5% CO_2 at 37°C.

For endothelial cell differentiation from hSKPs, SKPs were dissociated into single cells in Accumax (Innovative Cell Technologies) with 10 μM Y-27632(NACALAI TESQUE, INC) to avoid apotosis, and then suspended at a cell density of 1×10^6 cells per cm^2. Clonal hSKPs were plated and cultured on 0.1% gelatin coated 35-mm dishes or similarly coated type I atelocollagen sheets (Koken). The cells were cultured for 1week under a humidified atmosphere of 5% CO_2 at 37°C in CEIM.

Immunocytochemistry

Immunocytochemical analyses of cultured cells and fresh cornea samples were performed as described previously [32, 33]. In brief, samples were fixed at room temperature for 10 minutes in 4% formaldehyde in PBS. After three washes with PBS, samples were incubated for 15 minutes in Morphosave (Ventana Medical Systems, Inc., Tucson, Arizona, http://www.ventana.com). After another two washes with PBS, the samples were incubated for 30 minutes in 10% normal donkey serum to block nonspecific binding. This was followed by overnight incubation at 4°C with 1:200-diluted mouse anti-Na, K-ATPase α1 subunit antibody (Novus Biologicals, Littleton, CO, http://www.novusbio.com) or 1:200-diluted rabbit anti-ZO-1 antibody (Invitrogen) or 1:200-diluted rabbit anti-NGF Receptor p75 antibody (Merck Millipore, Darmstadt, Germant, http://www.merckmillipore.com/) or 1:200-diluted rabbit anti-CDH2 antibody (Novus Biologicals) with 1:200 diluted rabbit anti-Ki-67 antibody (Spring Bioescience, Pleasanton, CA, http://www.springbio.com/), or 1:200-diluted mouse anti-Nuclei antibody (Abnova, Taipei City, Taiwan, http://www.abnova.com/) and then washed 3 times in PBS. The samples were then incubated for 2 hours in a 1:200 dilution of Cy3-conjugated donkey anti-mouse IgG antibody (Jackson Immuno Research Laboratories, West Grove, PA, http://www.jacksonimmuno.com, final concentration of 30 mg/ml) or Cy3-conjugated donkey anti-rabbit IgG antibody (Jackson Immuno Research Laboratories) or Alexa Flour 488 conjuncted donkey anti-rabbit IgG antibody (life technologies), and washed three times in the dark. Finally, the samples were mounted on dishes with an anti-fading mounting medium containing 4′,6-diamidino-2-phenylindole ([DAPI] 1 mg/ml, Dojindo Laboratories, Kumamoto, Japan, http://www.dojindo.com). Images were obtained by fluorescent microscopy (Axio imager; Carl Zeiss, Inc., Weimar, Germany, http://www.zeiss.com) or confocal microscopy (LSM700; Carl Zeiss Inc.).

RT-PCR, qPCR Analysis

Total RNA was purified with the use of RNeasy kit (Qiagen, Hilden, Germany, http://www.qiagen.com) and cDNA was synthesized from total RNA using the Rever Tra Ace cDNA Synthesis Kit (TOYOBO Co., Ltd., Osaka, Japan, http://www.toyobo-global.com), according to the manufacturer's instructions. Polymerase chain reaction (PCR) was performed using Verti Thermal Cycler (Applied Biosystems, Thermo Fisher Scientific Inc.). Quantitative real time PCR with the Thunderbird SYBR qPCR Mix (TOYOBO) was performed using the Step One real-time PCR system (Applied Biosystems) in duplicate or triplicate. Primer sequences used are listed in previous reports [9, 15, 31].

Western Blotting

Mouse SKPs and sTECE were washed with PBS twice, and dissolved in a lysis buffer (M-PER; Thermo Fisher Scientific Inc.) with a protein inhibitor cocktail (Thermo Fisher Scientific Inc.). Western blot analysis was done with primary antibodies for β-actin (Abcam, Cambridge, U.K., http://www.abcam.com), Na, K-ATPase α-subunit (Epitomics, Inc., Burlingame, CA, http://www.epitomics.com), Pitx2 (Santa Cruz Biotechnology, Dallas, Texas, http://www.scbt.com) and N-cadherin (Novus Biologicals). Chemiluminescence images were analyzed using a Charge-Coupled Device camera system (ImageQuant LAS 4000; GE Healthcare, Little Chalfont, U.K., http://www.gehealthcare.com).

In Vitro Measurement of Pump Function by Ussing Chamber

The pump function of confluent monolayers of each cell type was measured with the use of the Ussing chamber as described previously [25, 32]. To standardize measurement conditions, each group was cultured for 1 week, and then an additional 48 hours after cells became confluent. The cells on Snapwell inserts were held by a specific holder (P2302), whose measurement area was 1.12 cm^2. Snapwell inserts (Transwell, Costar 3801, Corning Incorporated.) were then placed in an Ussing chamber (EMCSYS-2; Physiologic Instruments, San Diego, CA, http://www.physiologicinstruments.com). The endothelial cell surface side was in contact with one chamber, and the Snapwell membrane side was in contact with the other chamber. The chambers were carefully filled with Krebs-Ringer bicarbonate solution (120.7 mM NaCl, 24 mM $NaHCO_3$, 4.6 mM KCl, 0.5 mM $MgCl_2$, 0.7 mM Na_2HPO_4, 1.5 mM NaH_2PO_4, and 10 mM glucose) and bubbled with a mixture of 5% CO_2, 7% O_2, and 88% N_2 to pH 7.4. The chambers were maintained at 37°C by an attached heater. The short-circuit current (SCC) was sensed by narrow polyethylene tubes positioned close to both sides of the Snapwell filled with Krebs-Ringer solution and 4% agar gel, connected to silver electrodes. These electrodes were connected to a computer through the Ussing system (EVC4000: Physiologic Instruments Inc, San Diego, CA, http://www.

Stem Cells Translational Medicine published by Wiley Periodicals, Inc. on behalf of AlphaMed Press

physiologicinstuments.com) and the iWorx IX/408 data acquisition system (iWorx Systems Inc., Dover, NH, http://www.iworks.com) SCC was recorded by the Labscribe 2 Software for Research (iWorx Systems). After continuously monitoring for at least 10 minutes until SCC reached a steady state, the cells on the Snapwell membrane were loaded with 1mV currents through electrodes three times, and the SCC change was recorded.

Trans-endothelial resistance (TER) was calculated from the average SCC change and loaded voltage according to Ohm's law. Then, the specific Na, K-ATPase inhibitor, ouabain (final concentration; 10 mM. Sigma Aldrich) was added to the cell surface-side chamber. SCC was continually recorded during this procedure. The SCC attributable to Na, K-ATPase activity was calculated as the difference in SCC measured before and after the addition of ouabain. Finally, the SCC attributable to Na, K-ATPase activity was calculated as the potential difference (PD) by multiplying TER.

In Vivo Transplantation of sTECE Cell Sheets into a Rabbit Model of Bullous Keratopathy

Prior to transplantation, cell density of TECE cultured on carrier type I atelocollagen sheets (CM6, Koken) were manually counted by a microscope. Japanese white rabbits (female, 2.5 kg bodyweight; Shiraishi Animals Co. Ltd, Koshigaya, Japan, ks@sla-c.jp) were anesthetized intravenously with a mixture of diazepam (0.5 mg/kg; Takeda Pharmaceutical Company Limited, Osaka, Japan, http://www.takeda.com) and pentobarbital sodium (30 mg/kg; Kyoritsu Seiyaku Corporation, Tokyo, Japan, http://www.kyoritsuseiyaku.co.jp/english). Corneal transplantation was performed on the left eye of each animal as reported previously [9]. Briefly, corneal buttons were prepared by 8.0 mm Barron donor cornea punch (Barron Precision Instruments L.L.C., Grand Blanc, MI, http://www.bpic.com) from the center of donor corneas purchased from Funakoshi Co., Ltd., and Descemet's membrane along with the entire endothelium was stripped from the corneal buttons. sTECE cells cultured on carrier collagen sheets were harvested by a same size punch and immediately placed on the stromal bed. The sheets were attached to the stroma using forceps. The recipient central cornea was excised by Hessburg-Barron Vacuum Trephine (Barron Precision Instruments L.L.C.), and the corneal buttons with sTECE cell sheets or control corneal buttons without cells were then placed on the graft bed of the originally surgically operated eye and sutured with 16 interrupted sutures (10–0 nylon). Antibiotics (0.3% ofloxacin) and steroids (0.1% betamethasone) were applied topically 3 times a day. After transplantation, eyes were carefully observed by slit-lamp microscopy, and serial photographs were obtained. Central corneal thickness was measured with an ultrasound pachymeter (Tomey Corporation, Nagoya, Japan, http://www.tomey.com), and intraocular pressure (IOP) was measured by the Accupen (Accutome, Inc., Malvern, PA, http://www.accutome.com) on 1, 2, 5, and 8 days after transplantation. Central corneal thickness measurement and IOP measurement were performed by two different investigators who were masked to the details of transplantation in each group. Four eyes from four individual rabbits were used for each experimental group. Finally, 8 days after surgery, rabbits were sacrificed, and the operated eyes were enucleated, and the corneas of each operated eye were cut and paraffin-embedded, and mounted on dishes or glass slides with an anti-fading mounting medium containing DAPI. Localization of murine transplanted cells labeled by Wnt-1 Cre-/Floxed EGFP was observed by the Axio Imager (Carl Zeiss, Inc.). Localization of human transplanted cells labeled by anti-human nulcei antibody.

SA-β-Gal Staining

To evaluate senescence status, we performed senescence-associated expression of β-galactosidase (SA-β-Gal) staining using Senescence Detection Kit (BioVision Incorporated, Milpitas, CA, http://www.biovision.com/)

Statistical Analysis

Data are presented as mean ± SD and were compared by Student's *t* test or multiple *t* test with Bonferroni correction after ANOVA with the use of Excel 2013 software (Microsoft Corporation, Redmond, WA, https://www.microsoft.com/). A p value of $< .05$ was considered statistically significant. qRT-PCR analysis was performed using Step One software, version 2.3 (Applied Biosystems, Foster City, CA), and the results are presented as mean values with error bars representing 95% confidence intervals.

Results

Murine SKPs Differentiated Into Corneal Endothelium In Vitro

To ask if SKPs could differentiate into corneal endothelium, murine SKPs derived from facial skin of neonatal mouse were isolated. SKPs were then cultured in non-adhesive culture plates in EGF/FGF containing medium to form spheres (Fig. 1A). RT-PCR confirmed that the isolated cells expressed SKPs markers as well as neural crest markers (Supporting Information Fig. 1A).

We then compared morphological changes in cells cultured in corneal endothelium inducing medium [9]. When SKPs were cultured in DMEM/F12 medium without any other supplements, cells expressed fibroblastic morphology. These cells lost their ability to form cobblestone appearance of corneal endothelial cells. However, when SKPs were cultured in CEIM for a week, the cells formed a monolayer with a corneal endothelial-like cobblestone pattern (Fig. 1B).

To evaluate the differentiation of SKPs into corneal endothelium, we first assessed several series of corneal endothelial markers such as *Atp1a1* (Na,K-ATPase α-subunit), *Pitx2*, *Cdh2* (N-cadherin), *Slc4a4* (Na,HCO3 cotransporter), *Col4a2* (collagen type IV), and *Col8a2* (collagen type VIII) as corneal endothelium markers. SKPs-TECE was shown to express these series of markers by RT-PCR (Fig. 1C). Then, to assess whether corneal endothelial induction altered gene expression, we compared markers before and after differentiation by quantitative real-time reverse transcriptase polymerase chain reaction (qRT-PCR). Messenger RNA levels for *ATP1a1, Cdh2, Pitx2, Slc4a4, Collagen 4a2, and Collagen 8a2* were assessed. Relative to control SKPs, significant increase was observed in mRNA levels in the sTECE group (Fig. 1D). We further confirmed protein expression of these genes by Western blot analysis. Western blots showed that SKPs-TECE expressed higher protein levels of Na, K-ATPase α subunit, PITX2, and CDH2 compared to SKPs before induction (Fig. 1E). Immunocytochemistry analysis revealed sTECE expressed the tight junction marker ZO1 and the component of the corneal endothelial pump, Na, K-ATPase on the lateral side of the cells similar to control murine corneal endothelium (Fig. 1F). sTECE were similar to naïve corneal endothelium in the cell shape, nuclear cytoplasm ratio. However, cell size of sTECE is 0.7-fold smaller than corneal endothelium (Fig. 1F).

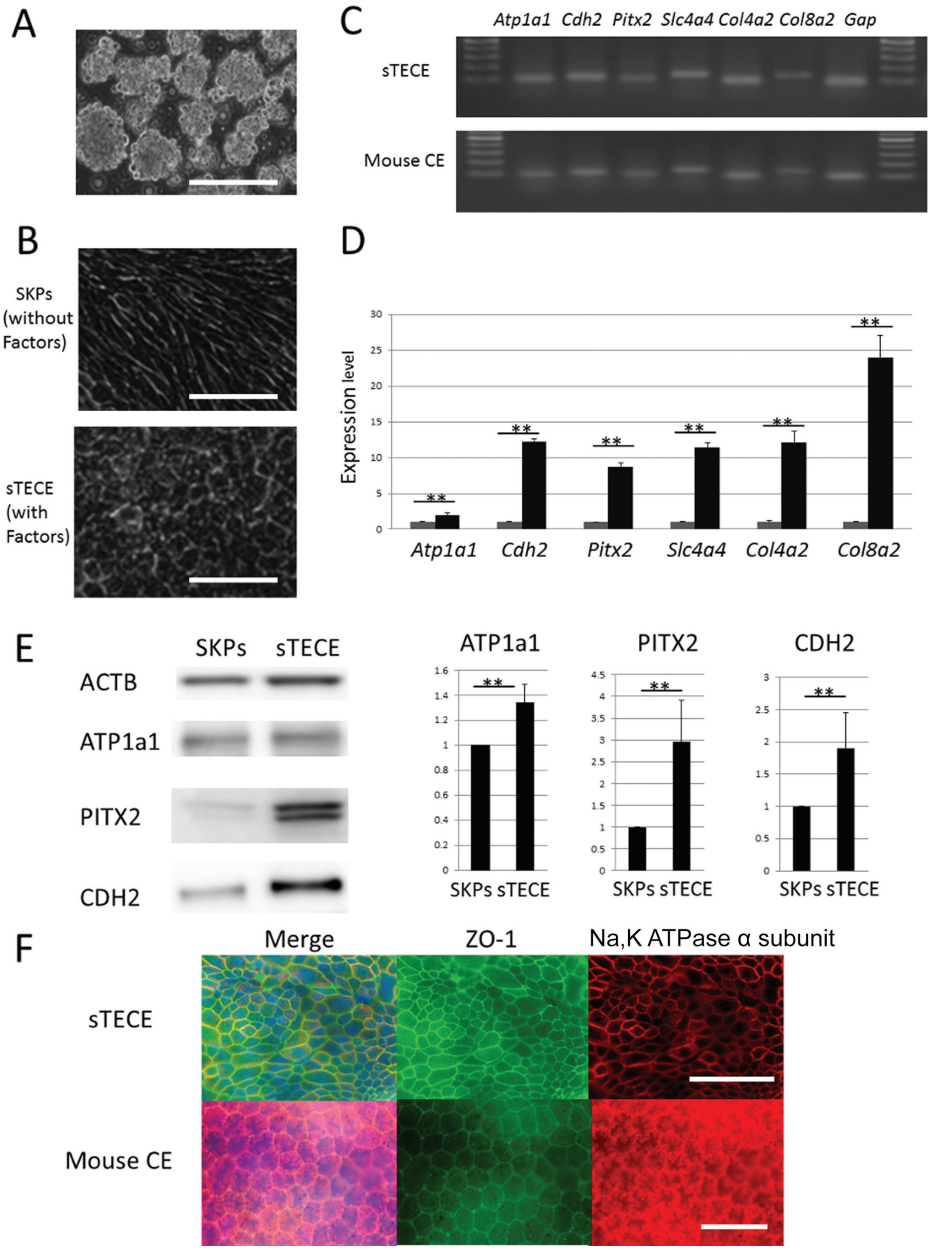

Figure 1. Isolation of SKPs and corneal endothelial induction. **(A)**: SKPs were successfully isolated and maintained in floating culture. **(B)**: Morphological changes without inducing factors exhibit a fibroblastic phenotype (upper panel), in contrast to sTECE that have a cobblestone appearance (lower panel). **(C)**: RT-PCR showed that sTECE expressed a series of corneal endothelial markers, *Atp1a1*, *Cdh2, Pitx2, Slc4a4, Col4a4, and Col8a2* (upper panel), similar to positive controls of murine corneal endothelial cells (lower panel). **(D)**: Comparison of qRT-PCR analysis of corneal endothelial markers before (left) and after (right) corneal endothelial induction. qRT-PCR showed that all markers were upregulated after endothelial induction. **(E)**: Western blots of ATP1a1, PITX2, and CDH2. Semiquantitative analysis shows significant upregulation at the protein level. **(F)**: Immunohistochemistry of ZO1 (green) and Na, K-ATPase (red) in sTECE (upper panel) was similar to mCE control (lower panel). Data expressed as mean ± SD of three replicate experiments. (D, E; Student's *t* test) Scale bars = 100 μm (A, F). Abbreviations: CDH2, cadherin type 2; mCE, mouse corneal endothelium; SKPs, skin-derived precursors; sTECE, SKPs derived tissue engineered corneal endothelium; ZO-1, zonular occluding-1.

To demonstrate the proliferative potential of sTECE, we performed Ki67 staining and found that a fraction of cells retain proliferative capacity (Supporting Information Fig. 1B). The N/C ratio of cells was 0.29 ± 0.12. We also confirmed that cultivation of sTECE can be maintained for up to 1 month (Supporting Information Fig. 1E). We were able to passage sTECE at least once, however, further passages can change corneal endothelial-like morphology into fibroblastic phenotype (Supporting Information Fig. 1D). To assess the senescence status of sTECE, we performed SA-β-Gal (Senescence-associated expression of β-galactosidase) staining and found that very few cells were positive (Supporting Information Fig. 1C).

Sphere Culture and Immunofluorescence Staining of Wnt1-Cre/Floxed-EGFP Derived SKPs and TECE

To confirm the derivation of SKPs from cranial neural crest cells, we isolated SKPs from Wnt1–Cre/Floxed EGFP mouse, since Wnt1-Cre is widely used in neural crest specific Cre driver lines

Stem Cells Translational Medicine published by Wiley Periodicals, Inc. on behalf of AlphaMed Press

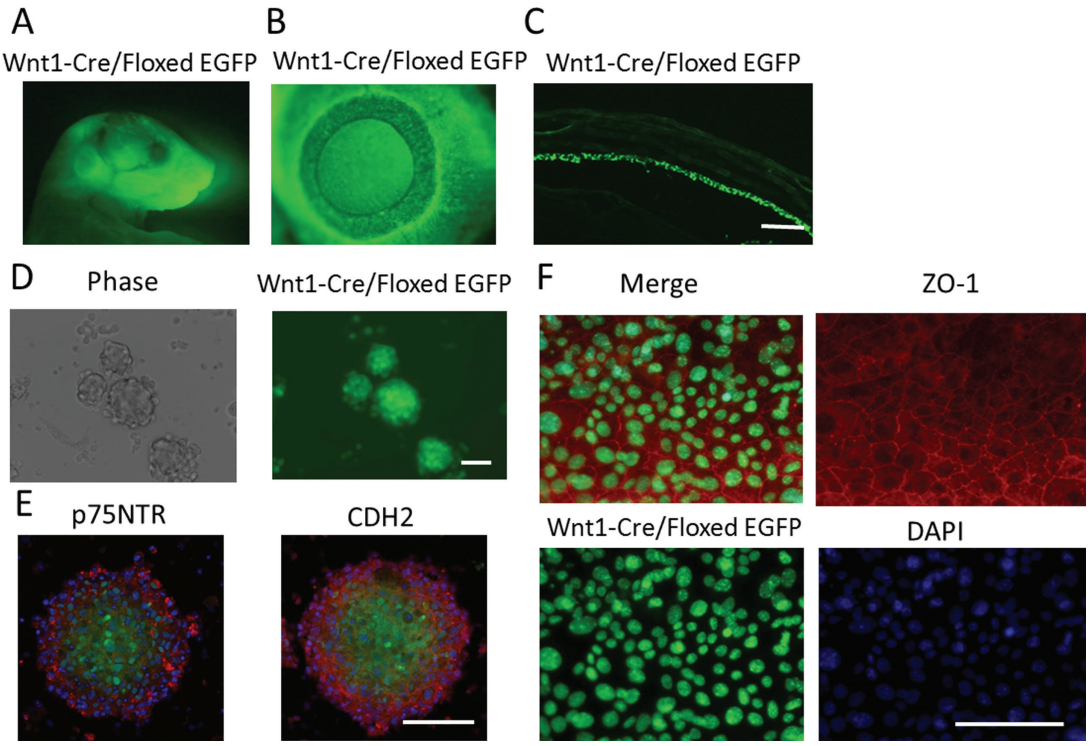

Figure 2. Immunofluorescence staining of Wnt1-Cre/Floxed-EGFP derived skin-derived precursors (SKPs) and tissue corneal endothelial-like cells (TECE). **(A)**: Wnt1-Cre/Floxed-EGFP mice show fluorescence in neural crest-derived tissue. **(B)**: Magnified view of the cornea shows EGFP positive cells (green) in facial skin as well as the corneal endothelium and stroma. **(C)**: Cryosection of Wnt1-Cre/Floxed-EGFP (day14) mouse cornea reveals positive staining (green) in corneal endothelium. **(D)**: SKPs derived from Wnt1-Cre/Floxed EGFP mice were maintained by sphere culture. Spheres were EGFP positive, confirming that facial skin-derived SKPs were of neural crest-origin. **(E)**: SKPs spheres expressed neural crest markers p75NTR (red) and CDH2 (red). **(F)**: TECE derived from spheres were all EGFP-positive, and expressed ZO-1 (red) along the cell boarders. Nuclei were labeled with DAPI (blue). Scale bar: 100 μm (C, F). Scale bar: 50 μm (D, E). Abbreviations: DAPI, 4′,6-diamidino-2-phenylindole; CDH2, cadherin type 2 N-cadherin; mCE, mouse corneal endothelium; p75NTR, p75 neurotrophin receptor; ZO-1, zonular occluding-1.

[26]. Fluorescent microscopic observation showed that EGFP–positive cells were expressed in the facial skin (Fig. 2A), iris and cornea (Fig. 2B) indicating neural crest origin. The corneal endothelium showed prominent linear staining along the interior boarder of the cornea (Fig. 2C). SKPs were successfully isolated from facial skin of this transgenic mouse. Isolated SKPs formed spheres and were 100% EGFP positive (Fig. 2D). These expression patterns confirmed data in previous reports [9, 18, 33]. The expression of p75NTR and CDH2, typical neural crest markers, were examined in spheres by immunostaining. The results show that both P75NTR (Fig. 2E left panel) and CDH2 (Fig. 2F right panel) were localized in the sphere. We next differentiate SKPs from this transgenic mouse into corneal endothelial phenotype according to protocol. Tissue engineered corneal endothelium derived from Wnt1-Cre/Floxed EGFP mouse SKPs expressed the tight junction marker, ZO1 in the lateral side of the cells, and also expressed EGFP fluorescence in all cells (Fig. 2F).

In Vitro Functional Analysis of Na, K-ATPase of SKPs-Derived Corneal Endothelial Cells Revealed Relatively High Pump Function

One of the most important functions of the corneal endothelium is Na-K, ATPase pump function. We therefore asked whether SKPs-derived corneal endothelium (sTECE) has high pump function compared to native corneal endothelium. Figure 3A shows Na,K-ATPase pump function measured by Ussing chamber in cultured mouse corneal endothelial cells (mCEs), 3T3 cells, SKPs (with 5% fetal bovine serum) and sTECE.

Figure 3B shows the total SCC changes, while Figure 3C shows the ouabain dependent SCC, which was calculated before and after addition of ouabain. As expected, SCC of mCEs (76.90 ± 13.96 $\mu A/cm^2$) was 5 times larger than 3T3 cells (17.08 ± 7.71 $\mu A/cm^2$). SKPs cultured with 5% FBS only was 2 times higher than 3T3 cells (33.832 ± 31.20 $\mu A/cm^2$). In contrast, SCC of sTECE (175.33 ± 46.11 $\mu A/cm^2$) was approximately 10 times larger than 3T3 cells. Figure 3D shows the total potential differences in each cell type. The ouabain-dependent potential difference attributed to Na, K pump function is shown in Figure 4E, which basically correlates with Figure 4D. Induction of sTECE significantly increased pump function by more than threefold compared to original SKPs cultured without corneal inducing factors. TER revealed no significant changes among 3T3 cells (17.78 ± 2.74 Ω/cm^2), mCEs (15.97 ± 3.00 Ω/cm^2), SKPs (27.38 ± 3.64 Ω/cm^2), and sTECE (17.71 ± 2.57 Ω/cm^2).

In Vivo Transplantation of SKPs-Derived Corneal Endothelium Recovered Cornea Transparency in a Rabbit Model of Bullous Keratopathy

To ask whether sTECE can be used as a potential source for treatment of corneal endothelial dysfunction, we used a rabbit model of bullous keratopathy. SKPs were plated and cultured on 0.1% gelatin-coated type I atelocollagen sheets and then induced to sTECE (see the Materials and Methods section), and the collagen sheets with TECE were cultured for 1 week. Six murine sTECE sheets with a cell density of 1989.35 ± 324 cells per mm^2 and six

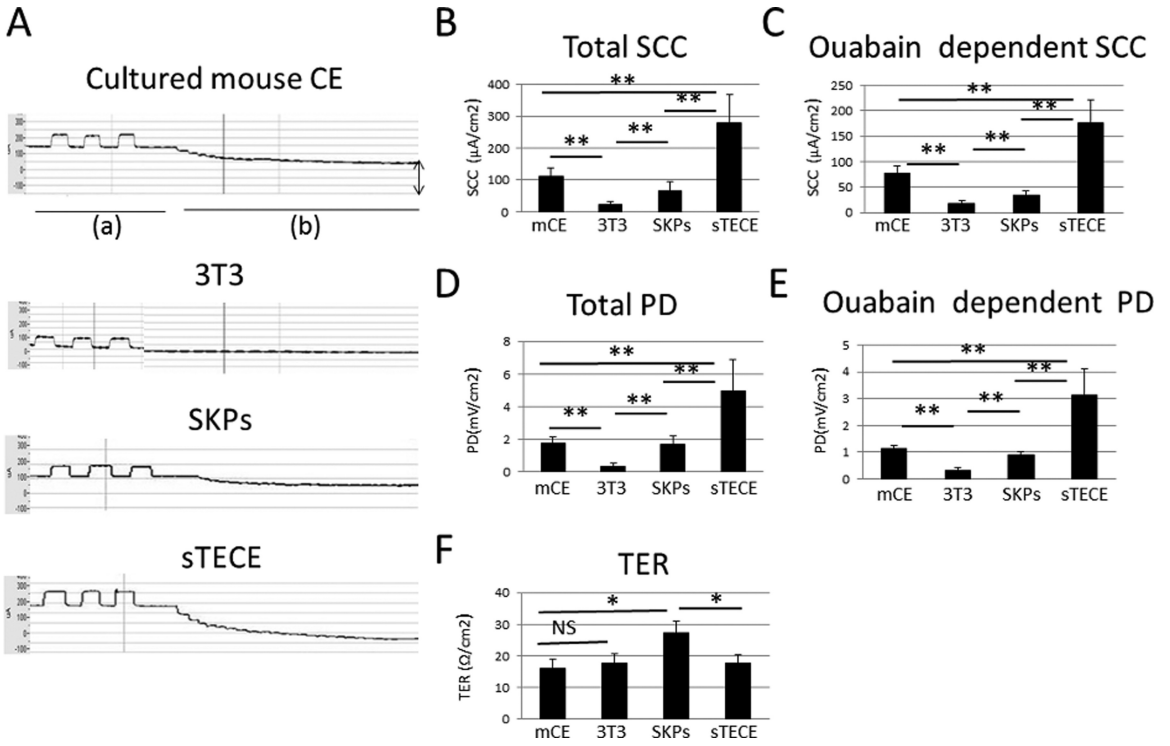

Figure 3. Measurement of pump function by the Ussing chamber system. **(A)**: Representative tracings of SCC in cultured mice CE, 3T3, SKPs, and sTECE. **(Aa)**: Represents the measurement of loaded voltage to calculate TER, **(Ab)**: Represents the influence of repeated ouabain addition until 10 mM. The arrow represents SCC changes before and after final Ouabain addition. **(B)**: Total SCC change. **(C)**: Ouabain dependent SCC calculated before and after ouabain addition. **(D)**: Total PD. **(E)**: Ouabain-dependent PD. (E) TER of cultured cell sheets. (B–F) Multiple *t*-test with BonFerroni correction after ANOVA. (**, $p < .01$; *, $p < .05$). Abbreviations: PD, potential difference; SKPs, skin-derived precursors; sTECE, SKPs derived tissue engineered corneal endothelium; SCC, short circuit current; TER, trans-epithelial resistance.

control grafts were transplanted to rabbit corneas by penetrating keratoplasty. Original corneal endothelium and Descemet's membrane were stripped from corneal buttons. sTECE on carrier collagen sheets were attached to the posterior surface of the donor buttons and transplanted with 16 interrupted sutures, whereas corneal buttons with neither corneal endothelium nor TECE sheets were transplanted in control eyes. Animals were assessed for evaluation by slit lamp examination, measurement of corneal thickness and IOP. Figure 4A shows slit lamp photographs of rabbit eyes 1, 5, and 8 days after transplantation. Corneas transplanted with sTECE were less edematous and maintained transparency (Fig. 4A: lower panel), whereas control eyes suffered severe corneal edema and thickened stroma (Fig. 4A: upper panel). Figure 4B shows corneal thickness change in three groups. During 8 days after transplantation, corneal thickness of control eyes increased over 1000 μm (1175.33 ± 69.24μm) and revealed severe corneal cloudiness consistent with bullous keratopathy, whereas sTECE-transplanted eyes maintained significantly lower corneal thickness than control eyes after 2 days to 8 days during the postoperative period (665.56 ± 95.65 μm). Figure 4C shows the changes in intra ocular pressure (IOP) during the observation period. IOP temporarily increased in control group as well as in sTECE transplanted group. However, IOP decreased gradually and maintained within the normal range of 10–20 mmHg. There was no significant difference between the three groups, indicating that the difference in corneal thickness was due to sTECE pump function, but not IOP. Figure 4D shows the whole mount photographs of sTECE-transplanted corneas. Wnt1-Cre/Floxed-EGFP derived florescence was detected only in the transplanted site inside the host-graft junctions at 8 days after transplantation.

Functional TECE Induced From hSKPs

We then asked whether this protocol could be used to differentiate hSKPs into functional TECE. hSKPs were successfully isolated from human eyelid skin from each donor. The 44-years-old and 82-years-old derived SKPs were used for further experiments (Fig. 5A, 5B) hSKPs were cultivated and expanded similar to murine SPKs. [31] SKPs were then maintained in sphere culture for at least a week, and P75NTR staining was confirmed (Supporting Information Fig. 2A). Consistent with the murine data, hSKPs cultured in medium with corneal inducing factors, showed cobble stone morphology (Supporting Information Fig. 2B). Human corneal endothelial markers *Atp1a1* (Na,K-ATPase α-subunit), *Cdh2* (N-cadherin) *Pitx2*, were upregulated after induction as shown by qRT-PCR (Fig. 5C). Immunohistochemical analysis confirmed positive staining of ZO1 and ATP1a1 α-subunit in human derived TECE (hTECE).

To demonstrate the proliferative potential of human skin derived precursors derived tissue engineered corneal endothelium (hTECE) we performed Ki67 staining and found that a fraction of cells showed proliferative capacity (Supporting Information Fig. 2D). We were able to maintain hTECE for at least a month in vitro (Supporting Information Fig. 2F). We were able to passage hTECE at least once, however consistent with murine data, further passages changed corneal endothelial-like morphology into fibroblastic phenotype (Supporting Information Fig. 2E). We also assessed the senescence status of hTECE with SA-β-Gal (Senescence-associated expression of β-galactosidase) staining and found positive staining in accordance with donor age (Supporting Information Fig. 2D).

Stem Cells Translational Medicine published by Wiley Periodicals, Inc. on behalf of AlphaMed Press

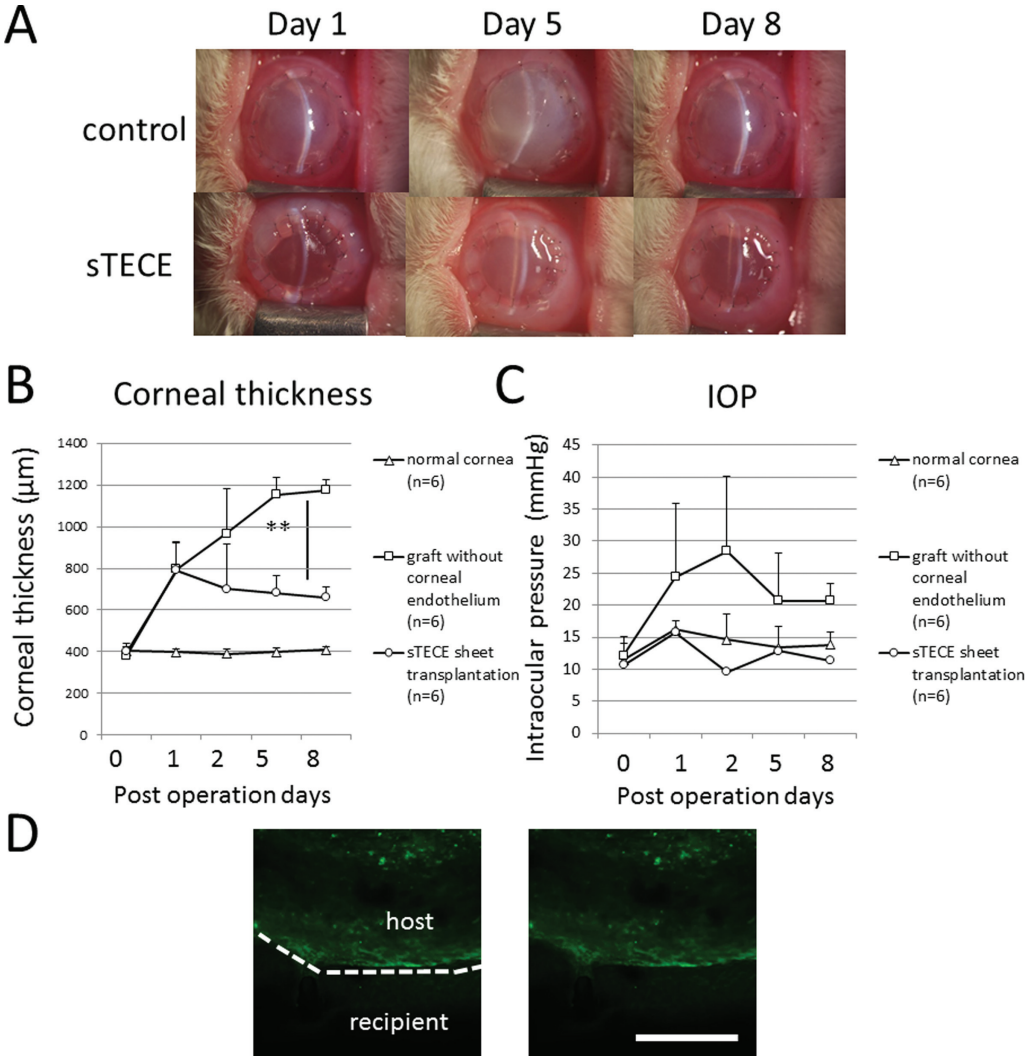

Figure 4. In vivo transplantation of mouse sTECE to rabbit cornea. **(A)**: Anterior segment photographs of rabbit cornea 1, 5, 8 days after transplantation. Control eyes transplanted with grafts without endothelium showed severe edema (upper panel), while grafts with sTECE remained transparent (lower panel). **(B)**: Change in corneal thickness after transplantation shows significant decrease in thickness due to edema in the sTECE group. **(C)**: IOP was similar in all groups indicating that the difference in corneal thickness was not due to differences in IOP. (Normal eyes: open triangles $n = 6$), (control eyes: open squares $n = 6$), (sTECE transplanted eyes: open circles, $n = 6$), **, $p < .01$, multiple t test with Bonferroni correction after ANOVA). **(D)**: Host-graft junction of harvested cornea 8 days after transplantation. EGFP positive cells showed fluorescence in the host cornea. Scale bar: 100 μm (D). Abbreviations: IOP, intraocular pressure; sTECE, SKPs derived tissue engineered corneal endothelium.

The pump function of confluent monolayers of hTECE, hSKPs with 5% FBS, and human corneal endothelial cell line (B4G12) were measured with the use of an Ussing chamber as described previously. The TER of hSKPs-TECE was 17.96 ± 4.16 (Ω/cm^2), control B4G12 was 8.86 ± 0.67 (Ω/cm^2). Na,K-ATPase pump activity of SKPs-TECE was calculated by the difference in SCC before and after Ouabain treatment. Na,K-ATPase pump activity of hSKPs-TECE was 2.64 ± 0.32 (mV/cm^2), hSKPs was 1.33 ± 0.38 (mV/cm^2), and control B4G12 was 0.79 ± 0.03 (mV/cm^2). hSKPs-TECE has significantly higher pump function (3.3-fold) compared to control B4G12 cells. (Fig. 5E)

To further investigate the function of hTECE in vivo, we transplanted hTECE sheets into the rabbit model of bullous keratopathy. Transplanted hTECE dramatically improved transparency (Fig. 5F). Corneas transplanted with hTECE were less edematous (Fig. 5F: lower panel), whereas control eyes suffered severe corneal edema and thickened stroma (Fig. 5F: upper panel). Figure 5G shows corneal thickness change in three groups. During 8 days after transplantation, corneal thickness of control eyes increased over 1000 μm (1185.33 ± 79.24 μm) and revealed severe corneal cloudiness consistent with bullous keratopathy, whereas hTECE-transplanted eyes ($N = 4$) maintained significantly lower corneal thickness than control eyes after 2 days to 8 days during the postoperative period (561.52 ± 112.12 μm) throughout the postoperative period. Figure 5H shows the changes of intra ocular pressure (IOP) during the observation period. IOP temporarily increased in control group as well as in hTECE transplanted group. However, IOP gradually decreased to the normal range of 10–20 mmHg. There was no significant difference between the three groups, indicating that the difference in corneal thickness was due to hTECE pump function. Figure 5I shows the whole mount photographs of hTECE-transplanted corneas. Anti-human nuclei antibody-derived florescence was detected only in the transplanted site inside the host-graft junctions at 8 days after transplantation.

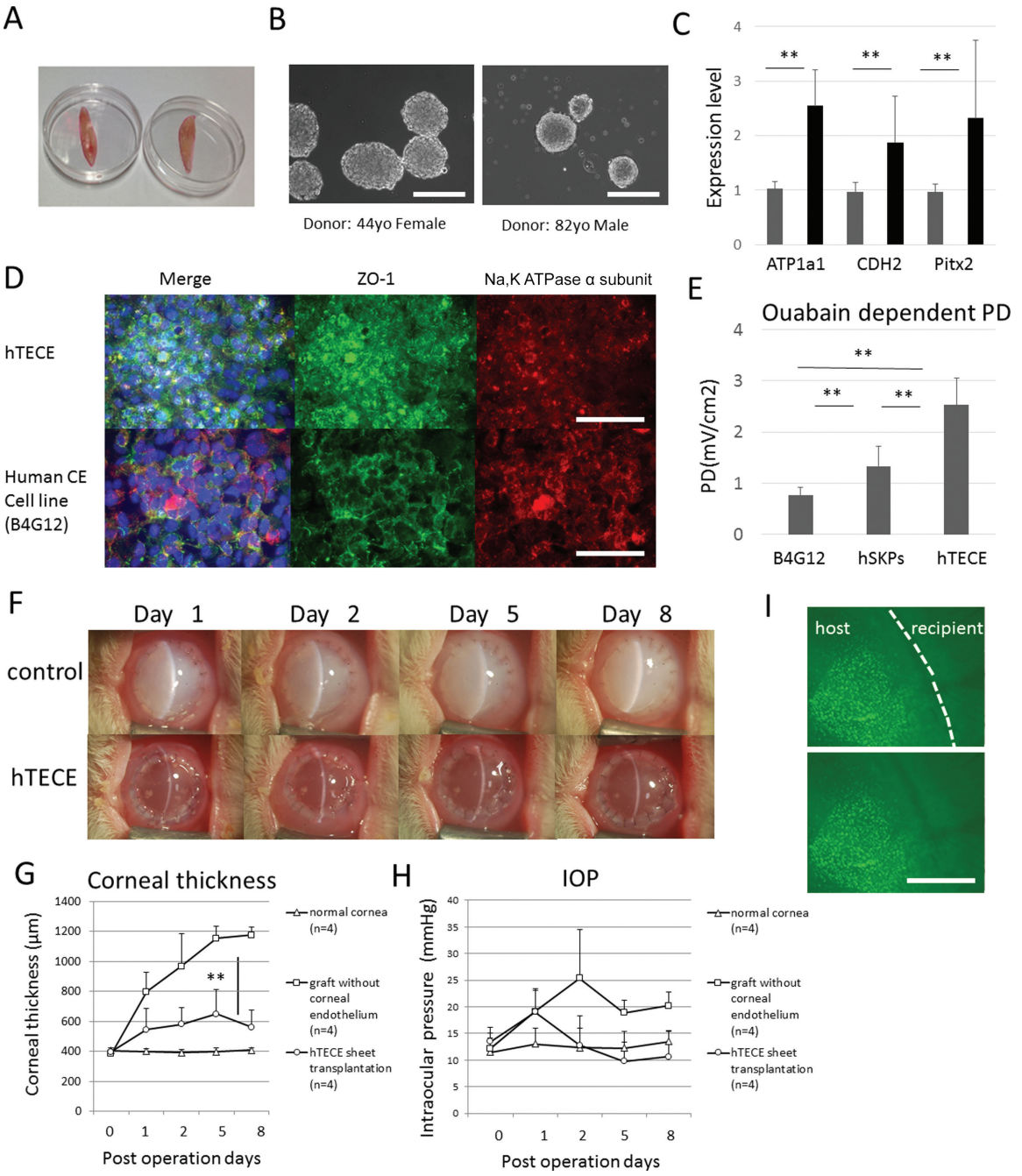

Figure 5. Functional TECE induced from human SKPs. **(A)**: Photograph of eyelid skin samples acquired during oculoplastic surgery. **(B)**: Human SKPs were successfully isolated in sphere culture. SKPs sphere derived from a 44-year-old female (left panel), and from an 82-year-old male (right panel). **(C)**: Real time RT-PCR show that corneal endothelial markers (*ATP1a1, CDH2, Pitx2*) were upregulated after endothelial induction (Left bar: before induction, right bar: after induction) Student's *t* test (**, $p < .01$). **(D)**: Immunohistochemistry of ZO1 (green) and Na, K-ATPase (red) in hTECE (upper panel) was similar to control human corneal endothelial cell line (B4G12) (lower panel). Nuclei were labeled with DAPI (blue). **(E)**: Ouabain-dependent PD. hTECE showed significantly higher PD compared to hSKPs or B4G12 cells (Student's *t* test **, $p < .01$). **(F)**: In vivo transplantation of hTECE to rabbit cornea. Anterior segment photographs of rabbit cornea 1, 2, 5, 8 days after transplantation. Control eyes transplanted with grafts without endothelium showed severe edema (upper panel), while grafts with sTECE remained transparent (lower panel). **(G)**: Change in corneal thickness after transplantation shows significant decrease in thickness in the hTECE group (normal eyes: open triangles $n = 4$), (control eyes: open squares $n = 4$), (hTECE transplanted eyes: open circles, $n = 4$), **, $p < .01$, multiple *t* test with Bonferroni correction after ANOVA). **(H)**: Change in IOP was similar in all groups indicating that the difference in corneal thickness was not due to difference in IOP. **(I)**: Host-graft junction of harvested cornea 8 days after transplantation of hTECE. Anti-human Nuclei antibody (EGFP) was stained only in the transplantation site. Scale bar: 50 μm (B), Scale bar: 100 μm (C), Scale bar: 200 μm (I). Abbreviations: hTECE, TECE from human SKPs; IOP, intraocular pressure; hSKPs, human SKPs; ZO1, zonular occluding-1; hCE, human corneal endothelium; SKPs, skin-derived precursors; TESE, tissue engineered corneal endothelium.

Stem Cells Translational Medicine published by Wiley Periodicals, Inc. on behalf of AlphaMed Press

Discussion

Recent advances in stem cell research and culture techniques have opened doors to a new field of cell therapy techniques for corneal endothelial regeneration. Several groups have reported the in vitro and in vivo differentiation of corneal endothelium from different stem cell sources. Ju et al reported the differentiation of corneal endothelial like-cell from rat neural crest cells in vitro [34]. Other stem cell sources such as ES cells [35], iPS cells [36], umbilical cord blood cells [37], and umbilical cord blood endothelial cells [38] also seem promising.

Our group previously reported derivation of functional tissue-engineered corneal endothelium from COPs cultivated from adult corneal stroma [9, 33]. COPs are similar to SKPs, a self-renewing, multipotent precursor isolated and expanded from the dermis of rodents and humans [10, 11]. Facial SKPs share a developmentally common origin with cornea endothelium, both of which come from the cranial neural crest. Therefore, facial SKPs may prove to be an accessible autologous source for potential use in stem cell therapy of the corneal endothelium. Using our previous protocol using retinoic acid and Wnt/ β catenin signaling, we successfully differentiated functional corneal endothelial cells from SKPs isolated from facial skin. As far as we know, this is the first report on the use of easily accessible, autologous source of stem cells for regenerating the corneal endothelium.

SKPs-derived TECE (sTECE) expressed a series of major corneal endothelial markers by RT-PCR. Of particular note was the upregulation of *Pitx2* mRNA and protein after endothelial induction, measured by qPCR and Western blots, respectively. *Pitx2* plays a crucial role in ocular development [24], along with signaling cross-talk of retinoic acid and Wnt/ β catenin. Our culture protocol shows that sTECE derivation mimics this developmental stage. However, unlike COPs, SKPs are derived from skin, a vascular rich tissue. SKPs are also reported to differentiate into α-smooth muscle [39], which may cause scarring of the cornea. Long-term observations are necessary to confirm that corneal clarity is not compromised.

Interestingly, in vitro analysis of pump function by the Ussing chamber revealed that sTECE had a pump function that was threefold higher than native corneal endothelial cells (3 mV). Undifferentiated SKPs also had measureable pump function (0.9 mV), which was lower than murine corneal endothelium (1.2 mV). According to our validation protocol for corneal endothelial regenerative medicine, we showed that 1 mV pump function was sufficient to maintain corneal transparency [25]. Therefore, sTECE shows more than enough pump function for clinical purposes.

We then demonstrated that sTECE functioned in an in vivo model of bullous keratopathy in rabbits to recover corneal transparency. This data shows that sTECE had sufficient pump function after transplantation into the eye. Furthermore, despite the fact that this was xenograft transplantation from mouse to rabbit, examinations showed no signs of immunological rejection, or neovascularization during the observation period. Secretion of trophic factors may be another mechanism by which sTECE confer regenerative effects. A previous report demonstrated that SKPs-derived Schwann cells transplanted into the spinal cord were able to modify the surrounding host environment [40].

One limitation of our study is the use of a rabbit model of bullous keratopathy. We used this model due to the established surgical technique and evaluation protocol used in a previous study [9, 25]. Since rabbit corneal endothelial cells proliferate and regenerate, long-term observation is not possible. However, the objective of this data was to show in vivo function using corneal thickness as a parameter, and to this end, we were successful in showing pump function in vivo. Another limitation is that we harvested neonatal murine facial skin, and not that of adult mice. However, our data shows the successful isolation of SKPs from aged human tissue, suggesting that age may not be a problem when isolating from human samples. In fact, hTECE derived from an 82-year-old adult human donor dramatically improved corneal edema in vivo. Although hTECE from this donor showed many SA-β-Gal positive cells suggesting cellular senescence, this did not seem to affect cell function. Since corneal endothelial cells do not need to proliferate in vivo, an aged autologous source may have benefits over a younger allogeneic donor. Cells can be obtained from redundant tissue surgically removed for cosmetic purposes, and therefore, ethical issues should not be a problem. SKPs are a promising source of cells for regenerative therapy since they can easily be harvested from peripheral parts of the body. This will make autologous transplantation possible [41], which will lower the barrier for safety regulatory issues. SKPs are also a safe source of tissue since there is no risk of tumorigenesis as with the case with pluripotent stem cells [42]. Further optimization of isolation and culture techniques of hSKPs are required prior to clinical use. The cornea is an ideal tissue to apply cell injection therapy due to the small number of cell required. Furthermore, the transparent nature of the cornea will allow direct visualization of transplanted cells, and quick intervention in cases of unexpected events.

Conclusion

We successfully induced functional corneal endothelial-like cells from facial SKPs that showed sufficient pump function in a rabbit model of corneal endothelial dysfunction. Our findings suggest that SKPs may be used as a source of autologous cells for the treatment of corneal endothelial disease.

Acknowledgments

We thank Dr. Shinji Ideta and Dr.Yu Ohta for supply of oculoplastic surgery skin samples. We thank Tomomi Sekiguchi, Miyuki Yasuda, Hiroko Niwano, Yuki Izawa and Kazuya Yamashita for technical assistance and Dr. Hideyuki Miyashita for general support. We thank Toru Tanaka from Carl Zeiss Microscopy Y.A.S.C. for technical assistance. We thank Dr. Narihito Nagoshi from Department of Orthopedic Surgery, Keio University School of Medicine and Dr. Motoko Naitoh from the Department of Plastic and Reconstructive Surgery, Kyoto University School of Medicine for useful suggestions. This work was supported by grants from Grants-in-Aid for Scientific Research from Japan Society for the Promotion of Science (JSPS) to Shigeto Shimmura and the Ministry of Education, Culture, Sports, Science and Technology of Japan (MEXT). (Grant Number: KAKENHI 24592644) The funders had no role in study design, data collection and analysis, decision to publish, or preparation of the manuscript.

Author Contributions

E.I.: Collection and assembly of data, manuscript writing; S.H. and K.H.: Collection and assembly of data; S.Y., H.O., and K.T.: Data analysis and interpretation; S. Shibata: Provision of study material; S. Shimmura. Conception and design, manuscript writing, final approval of manuscript.

Disclosure of Potential Conflicts of Interest

S. H., S. Y., K. T., and S. Shimmura have a patent (WO2013051722) pertaining to material in manuscript. H.O. is a paid Scientific Advisory Board of SanBio Co Ltd., but has no relevance to this article. All other authors indicate no potential conflicts of interest.

References

1 Bourne WM. Clinical estimation of corneal endothelial pump function. Trans Am Ophthalmol Soc. 1998;96:229–239; discussion 239–242.

2 Joyce NC. Proliferative capacity of the corneal endothelium. Prog Retin Eye Res 2003;22:359–389.

3 Hollingsworth J, Perez-Gomez I, Mutalib HA et al. A population study of the normal cornea using an in vivo, slit-scanning confocal microscope. Optom Vis Sci 2001;78:706–711.

4 Hatou S, Shimmura S, Shimazaki J et al. Mathematical projection model of visual loss due to fuchs corneal dystrophy. Invest Ophthalmol Vis Sci 2011;52:7888–7893.

5 Peh GS, Beuerman RW, Colman A et al. Human corneal endothelial cell expansion for corneal endothelium transplantation: An overview. Transplantation 2011;91:811–819.

6 Stevens GA, White RA, Flaxman SR et al. Global prevalence of vision impairment and blindness: magnitude and temporal trends, 1990-2010. Ophthalmology 2013;120:2377–2384.

7 Doyle JW, Smith MF. Glaucoma after penetrating keratoplasty. Semin Ophthalmol 1994;9:254–257.

8 Sellami D, Abid S, Bouaouaja G et al. Epidemiology and risk factors for corneal graft rejection. Transplant Proc 2007;39:2609–2611.

9 Hatou S, Yoshida S, Higa K et al. Functional corneal endothelium derived from corneal stroma stem cells of neural crest origin by retinoic acid and Wnt/beta-catenin signaling. Stem Cells Dev 2013;22:828–839.

10 Toma JG, Akhavan M, Fernandes KJ et al. Isolation of multipotent adult stem cells from the dermis of mammalian skin. Nat Cell Biol 2001;3:778–784.

11 Toma JG, McKenzie IA, Bagli D et al. Isolation and characterization of multipotent skin-derived precursors from human skin. Stem Cells 2005;23:727–737.

12 McKenzie IA, Biernaskie J, Toma JG et al. Skin-derived precursors generate myelinating Schwann cells for the injured and dysmyelinated nervous system. J Neurosci 2006; 26:6651–6660.

13 Krause MP, Dworski S, Feinberg K et al. Direct genesis of functional rodent and human Schwann cells from skin mesenchymal precursors. Stem Cell Rep 2014;3:85–100.

14 Lavoie JF, Biernaskie JA, Chen Y et al. Skin-derived precursors differentiate into skeletogenic cell types and contribute to bone repair. Stem Cells Dev 2009;18:893–906.

15 Fernandes KJ, McKenzie IA, Mill P et al. A dermal niche for multipotent adult skin-derived precursor cells. Nat Cell Biol 2004;6:1082–1093.

16 Fernandes KJ, Kobayashi NR, Gallagher CJ et al. Analysis of the neurogenic potential of multipotent skin-derived precursors. Exp Neurol 2006;201:32–48.

17 Fernandes KJ, Toma JG, Miller FD. Multipotent skin-derived precursors: adult neural crest-related precursors with therapeutic potential. Philos Trans R Soc Lond B Biol Sci 2008;363:185–198.

18 Nagoshi N, Shibata S, Kubota Y et al. Ontogeny and multipotency of neural crest-derived stem cells in mouse bone marrow, dorsal root ganglia, and whisker pad. Cell Stem Cell 2008;2:392–403.

19 Biernaskie J, Sparling JS, Liu J et al. Skin-derived precursors generate myelinating Schwann cells that promote remyelination and functional recovery after contusion spinal cord injury. J Neurosci 2007;27:9545–9559.

20 Chen Z, Pradhan S, Liu C et al. Skin-derived precursors as a source of progenitors for cutaneous nerve regeneration. Stem Cells 2012;30:2261–2270.

21 Jinno H, Morozova O, Jones KL et al. Convergent genesis of an adult neural crest-like dermal stem cell from distinct developmental origins. Stem Cells 2010;28:2027–2040.

22 Reneker LW, Silversides DW, Xu L et al. Formation of corneal endothelium is essential for anterior segment development - a transgenic mouse model of anterior segment dysgenesis. Development 2000;127:533–542.

23 Gage PJ, Rhoades W, Prucka SK et al. Fate maps of neural crest and mesoderm in the mammalian eye. Invest Ophthalmol Vis Sci 2005;46:4200–4208.

24 Evans AL, Gage PJ. Expression of the homeobox gene Pitx2 in neural crest is required for optic stalk and ocular anterior segment development. Hum Mol Genet 2005;14:3347–3359.

25 Hatou S, Higa K, Inagaki E et al. Validation of Na,K-ATPase pump function of corneal endothelial cells for corneal regenerative medicine. Tissue Eng Part C Methods 2013;19:901–910.

26 Danielian PS, Muccino D, Rowitch DH et al. Modification of gene activity in mouse embryos in utero by a tamoxifen-inducible form of Cre recombinase. Curr Biol 1998;8:1323–1326.

27 Kawamoto S, Niwa H, Tashiro F et al. A novel reporter mouse strain that expresses enhanced green fluorescent protein upon Cre-mediated recombination. FEBS Lett 2000;470:263–268.

28 Fernandes KJ, Miller FD. Isolation, expansion, and differentiation of mouse skin-derived precursors. Methods Mol Biol 2009; 482:159–170.

29 Belicchi M, Pisati F, Lopa R et al. Human skin-derived stem cells migrate throughout forebrain and differentiate into astrocytes after injection into adult mouse brain. J Neurosci Res 2004;77:475–486.

30 Joannides A, Gaughwin P, Schwiening C et al. Efficient generation of neural precursors from adult human skin: astrocytes promote neurogenesis from skin-derived stem cells. Lancet 2004;364:172–178.

31 Yoshikawa K, Naitoh M, Kubota H et al. Multipotent stem cells are effectively collected from adult human cheek skin. Biochem Biophys Res Commun 2013;431:104–110.

32 Inagaki E, Hatou S, Yoshida S et al. Expression and distribution of claudin subtypes in human corneal endothelium. Invest Ophthalmol Vis Sci 2013;54:7258–7265.

33 Yoshida S, Shimmura S, Nagoshi N et al. Isolation of multipotent neural crest-derived stem cells from the adult mouse cornea. Stem Cells 2006;24:2714–2722.

34 Ju C, Zhang K, Wu X. Derivation of corneal endothelial cell-like cells from rat neural crest cells in vitro. PLoS One 2012;7:e42378.

35 Zhang K, Pang K, Wu X. Isolation and transplantation of corneal endothelial cell-like cells derived from in-vitro-differentiated human embryonic stem cells. Stem Cells Dev 2014;23:1340–1354.

36 Fukuta M, Nakai Y, Kirino K et al. Derivation of mesenchymal stromal cells from pluripotent stem cells through a neural crest lineage using small molecule compounds with defined media. PloS One 2014;9:e112291.

37 Joyce NC, Harris DL, Markov V et al. Potential of human umbilical cord blood mesenchymal stem cells to heal damaged corneal endothelium. Mol Vis 2012;18:547–564.

38 Shao C, Chen J, Chen P et al. Targeted transplantation of human umbilical cord blood endothelial progenitor cells with immunomagnetic nanoparticles to repair corneal endothelium defect. Stem Cells Dev 2015;24:756–767.

39 Steinbach SK, El-Mounayri O, DaCosta RS et al. Directed differentiation of skin-derived precursors into functional vascular smooth muscle cells. Arterioscler Thromb Vasc Biol 2011;31:2938–2948.

40 Biernaskie J, Sparling JS, Liu J et al. Skin-derived precursors generate myelinating Schwann cells that promote remyelination and functional recovery after contusion spinal cord injury. J Neurosci 2007;27:9545–9559.

41 Nagoshi N, Shibata S, Nakamura M et al. Neural crest-derived stem cells display a wide variety of characteristics. J Cell Biochem 2009;107:1046–1052.

42 Nori S, Okada Y, Yasuda A et al. Grafted human-induced pluripotent stem-cell-derived neurospheres promote motor functional recovery after spinal cord injury in mice. Proc Natl Acad Sci USA 2011;108:16825–16830.

See www.StemCellsTM.com for supporting information available online.

Stem Cells Translational Medicine published by Wiley Periodicals, Inc. on behalf of AlphaMed Press